Applied Energy 145 (2015) 124–132

Contents lists available at ScienceDirect

Applied Energy

journal homepage: www.elsevier.com/locate/apenergy

ANN based MPPT method for rapidly variable shading conditions

Santi Agatino Rizzo *, Giacomo Scelba

Dipartimento di Ingegneria Elettrica, Elettronica e Informatica (DIEEI), University of Catania, Italy

HIGHLIGHTS

- MPPT for mobile installations where shading phenomena suddenly and frequently change.
- Irradiance distribution over the modules and their temperature is unknown (no sensor).
- The time required to esteem the maximum power point is small and fixed.
- The quality indices show the ANN structures with the best tradeoff accuracy-time.
- Good results in terms of robustness to parameter variations of PV system.

ARTICLE INFO

Article history:
Received 7 August 2014
Received in revised form 19 January 2015
Accepted 20 January 2015

Keywords:
Artificial neural networks
Maximum Power Point Tracking (MPPT)
Photovoltaic (PV)
Electric vehicles
Shading
Solar energy

ABSTRACT

This paper proposes a novel Maximum Power Point Tracking (MPPT) method suitable for any application in which very fast changing and not uniform shading conditions continuously occur, as in case of photovoltaic systems (PVs) installed in the roof of electric vehicles. Basically, an Artificial Neural Network (ANN) based approach is utilized to automatically detect the global maximum power point of the PV array by using a preselected number of power measurements of the PV system. The method requires only the measure of PV voltages and currents, thus avoiding the use of additional sensors providing information about the environmental operating conditions and temperature of PV modules. The time interval required to achieve the maximum power generation from the PV modules is about constant and established *a priori*. The greater the number of power–voltage characteristic scansions, the greater the ANN's ability to meet the maximum and its prediction accuracy. The algorithm is cost-effective, with no additional hardware requirements and limited dependence on system parameter variations. Numerical simulations have validated the effectiveness of the proposed method, and have highlighted the tradeoff between the preselected number of power–voltage characteristic scansions, the size of the ANN and its prediction accuracy.

1. Introduction

As it is well known, the use of photovoltaic systems (PV) are becoming more and more important due to their environment friendly and economically sustainable energy source, also in electric vehicles. On the other hand, the photovoltaic technology still faces efficiency limits, thus control techniques named Maximum Power Point Tracking (MPPT) have been proposed to optimally exploit the available power. These algorithms are tracking controls employed to extract the maximum power from PV modules depending on the array temperature, solar irradiation, shading conditions and PV cell ageing.

The most widely used MPPT methods can be grouped in two different categories: hill climbing methods, such as Perturb and Observer (P&O) and Incremental Conductance (INC), and constant voltage methods [1–4]. Starting from the standard implementations, other technical solutions [5–18] have been proposed in order to improve the accuracy and dynamic behavior of the tracking controls. On the other hand, most of them neglect that MPPT is a multimodal optimization problem [19] since there are local optima in the *P–V* characteristic curve when not uniform irradiance occurs over the photovoltaic system.

Considerable research efforts have been directed toward the development of more sophisticated MPPT algorithms able to identify the Global Maximum Power Point (GMPP) in order to extract the whole available power from the PV system under partially shaded conditions [20–33]. The computational burden, range of effectiveness and convergent speed of these algorithms is quite

* Corresponding author.
E-mail address: santi.rizzo@dieei.unict.it (S.A. Rizzo).

http://dx.doi.org/10.1016/j.apenergy.2015.01.077
0306-2619/

Nomenclature

V_{PV}, I_{PV}	PV array output voltage and current
R_s	resistance of the metallic contacts and ohmic resistance of the material
R_{sh}	resistance associated to the leakage of the current across the p–n junction or at the cell edges
q	electron charge
I_{ph_STC}, I_{ph}	photo-generated current in Standard Test Conditions (STC) and operating conditions
I_o	dark saturation current in STC
T_{STC}, T	temperature at STC and operating conditions
I_{SC_STC}	short circuit current measured at STC
A	diode quality (ideality) factor
k	Boltzmann's constant
n_p, n_s	number of cells connected in parallel and series
V_{oc_STC}, V_{oc}	open circuit voltage at STC and operating condition
G_{STC}, G	irradiance at STC and operating condition
V_T	thermal voltage
K_I, K_V	temperature coefficient of short-circuit current and temperature coefficient of open-circuit voltage

different and depends on the adopted theoretical methodology. Some methods determine the GMPP by exploiting deterministic searching algorithms such as constant power operation [21], dividing rectangles (DIRECT) method [22], restricted voltage window search algorithm [25], Cuckoo search [30], while other MPPT algorithms are based on metaheuristic approaches such as the particle swarm optimization [20] and Artificial Neural Networks (ANNs) [26]. More in general, in the field of multimodal optimization the Evolutionary Algorithms [34], e.g. genetic algorithms [35], applying niching strategies [36] are designed to properly address multimodal functions. Furthermore, some niching algorithms are coupled with Deterministic Methods (DMs) [37] to enhance the final solution accuracy [38]. The basic idea is to firstly search the global optimum using a niching algorithm and, then the DM starts from the provided solution to draw up to the actual optimum. Therefore, a further distinction among algorithms that can be adopted to MPPT concerns the number of stages that the MPPT algorithms use. In fact, some techniques track the GMPP by using a unique procedure, while other methods identify the GMPP by adopting two stages. The latter ones, firstly adopt an algorithm to identify the "hill" where the GMPP is potentially located, and then a further algorithm is employed to reach the GMPP. In this perspective, the use of metaheuristic approaches coupled with a DM seems a good solution provided that information about the solar irradiance distribution on the panels and/or their temperature as well as the knowledge of the system model are given. Actually, these techniques could be applied without the use of a model, but the approach becomes very harmful because each objective function evaluation calls for changing the PV voltage in order to measure the current.

Hence, the techniques mentioned so far require the measurement of solar radiation over the panel and their temperature, and/or the scansion of a large portion of the PV characteristic to suitably determine the GMPP. Consequently, the main limitation of the first kind of techniques is the necessity of using additional sensors and properly system models, whereas the main limitation of the second ones is the lost of energy owing to the time spent to sample the PV characteristic. In this perspective, in [39] a techniques based on the DIRECT search algorithm (first stage) and a suitable P&O algorithm (second stage) has been proposed. More in general, the aforementioned techniques have been designed for PV system placed in fixed installation, where the shading phenomena does not suddenly and frequently change as in case of installations on the roof of electric vehicles. In this case, a very accurate and fast GMPP tracking is necessary in order to maximize the extracted energy, taking into account that the PV system operates under the high probability that the solar irradiance on the panel is not uniformly distributed, especially due to the presence of other vehicles, buildings and any other obstacles that blocks or refracts the solar rays impacting the PV modules, and this distribution continuously changes meanwhile the vehicle moves in the traffic.

In order to overcome the aforementioned limitations, the paper aims to study the effectiveness of an ANN based MPPT approach whose goal is to quickly and accurately estimate the GMPP when no information about the solar irradiance distribution over the modules and their temperature is given, and when the PV system is subjected to continuously and rapidly changing shadowing patterns. Few measures are used to esteem the GMPP by means of the ANN, and they are set *a priori*. Consequently, the estimation time is small and fixed. In this work, the solution provided by the ANN is given, as starting point, to a zero-order P&O method, named as Pattern Search (PS) [37], in order to improve the accuracy of the esteemed maximum power point (EMPP). Therefore, differently from [39] the ANN is used to directly estimate the GMPP at first stage, while the P&O method is exploited only to refine the result. Finally, to evaluate the performance of various ANN's structures some quality indices are proposed, and the robustness of the proposed approach to parameter variations of PV system has been also assessed.

Actually, ANNs have been already applied to MPPT problems, but it is the first time that ANNs are used to identify the GMPP as proposed in this paper, far as authors know. The other ANN based MPPT algorithms presented in past literature are usually exploited to compensate the parameter variations occurring in the PV system in the identification of local MPPs [14–18]. On the other hand, the ANN based MPPT method presented in [32] estimates the GMPP by means of a single voltage and current measurement but the study is limited to a very restricted number of shading combinations, thus it is few practicable for a generic PV system especially when it is continuously subjected to very fast changing and not uniform shading conditions.

The paper is structured as follows: a brief description of the considered PV model is presented in Section 2, while Section 3 deals with the explanation of the entire proposed MPPT method; a detailed analysis of the ANN based MPPT method is described in Section 4, and a case study is investigated in Section 5; finally, some conclusions and future work are pointed out in Section 6.

2. PV system modeling

As mentioned in the previous section, a PV module can be analytically represented by its current vs voltage electrical characteristic, achieved by combining the solar cells in series and parallel. The characteristic curve is not linear because of operational physical phenomena.

Different analytical model of the PV system have been proposed in literature [40,41], and among of them a single diode model representation of each solar cell has been taken into consideration in the following analysis. The model is given by:

$$I_{PV} = n_p\left(I_{ph} - I_0\left[e^{\frac{q(V_{PV}+R_sI_{PV})}{AkTn_s}} - 1\right] - \frac{(V_{PV}+R_sI_{PV})}{n_sR_{sh}}\right) \quad (1)$$

$$I_{ph} = I_{ph\_STC} + K_I(T - T_{STC})\frac{G}{G_{STC}} \quad (2)$$

$$I_0 = \frac{I_{SC\_STC} + K_I(T - T_{STC})}{e^{(V_{oc\_STC}+K_V(T-T_{STC})/V_T - 1)}} \quad (3)$$

Relationships (1)–(3) clearly show the dependence of the model on the solar radiance and temperature conditions. Moreover, the degradation of the cells due to the outdoor conditions can affect the parameters included in (1)–(3).

Starting from this mathematical representation, the power curve associated to the PV array is obtained by considering the series and parallel connection of the PV modules.

Assuming to consider a PV array consisting of identical photovoltaic cells, under uniform solar irradiation, the typical *P–V* curve of the array includes a single peak, as depicted in Fig. 1.

When partial shading occurs in one of the cell composing the PV module, the last reduces the current circulating through the unshaded cells, causing the so called hot-spot heating and thus the crack of the shaded cell [28]. This drawback is overcome by using an external bypass diode conducting every time the solar cell is reversed biased, allowing the current of unshed cells to flow externally to the shaded cell, thus preventing the hot-spot damages. A similar approach is applied at module level. Although the impact of shaded cells can be mitigated by inserting bypass diodes, partial shading still significantly impairs the energy produced from the PV system due to two reasons: the *P–V* curve presents multiple peaks and the position and amplitude of the global maximum change as the shading conditions change. Fig. 1 highlights these two aspects by showing the *P–V* characteristic of a PV array under uniform and partially shaded operating conditions.

The main goal of the following sections is to present a novel MPPT implementation able to extract the maximum allowable power from the PV array even when sudden and recurring shading condition variations take place.

3. Maximum power point searching method

The proposed MPPT method consists of two different procedures, which are activated by using one technique proposed in literature [42]. A flowchart of the entire MPPT method is reported in Fig. 2. The voltage and current are measured at the PV array terminals with

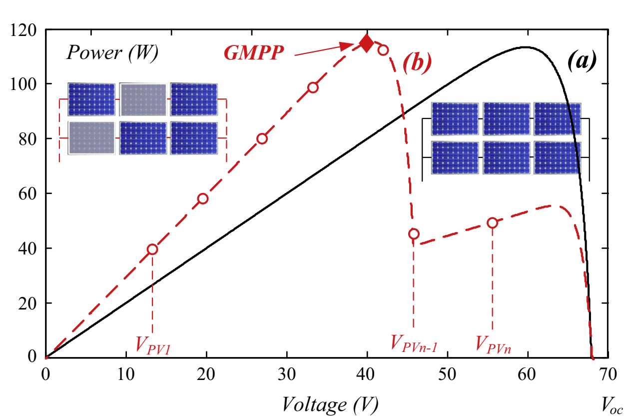

Fig. 1. Example of *P–V* characteristic of a PV array (a) under uniform irradiation and (b) shading distribution.

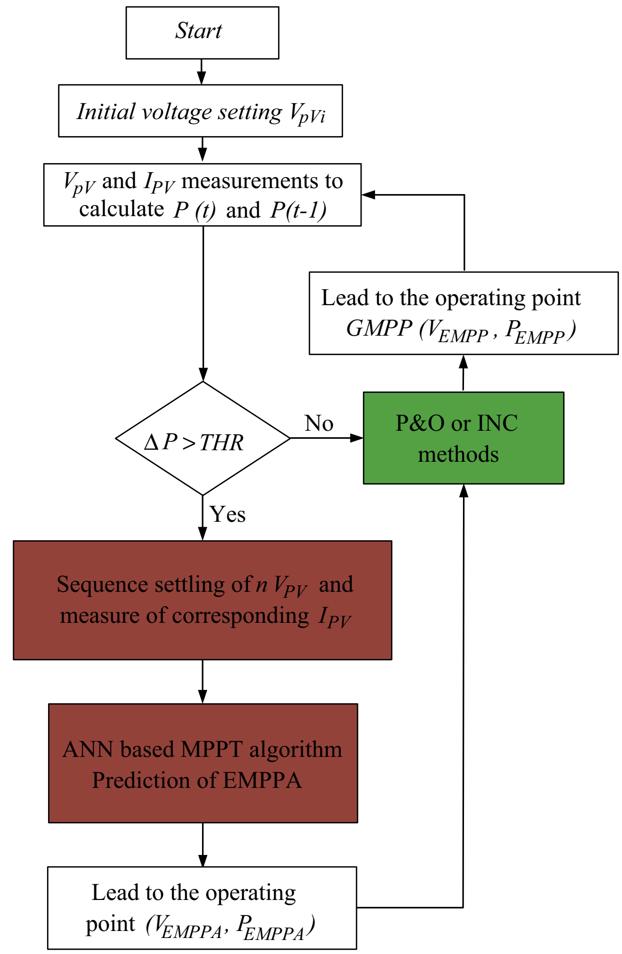

Fig. 2. Flowchart of the proposed MPPT method.

a sampling time ΔT of few seconds. Hence, it is expected that the calculated output power variation ΔP is greater than a suitable threshold THR (e.g. 0.1–0.2P_{EMMP}) when the insolation distribution changes. Significant power variations with uniform insolation are unlikely for the considered ΔT.

Whenever the power variation is limited under a certain threshold THR, it is assumed that the *P–V* curve maintains the same shape and the tracking of the Maximum Power Point (MPP) is performed by using a local method: the PS. In case the threshold is overcome, the ANN based method is applied, followed by the local MPPT method. In particular, whenever the proposed ANN based MPPT method is activated, the power converter connected to the PV array terminals forces it to sequentially operate at *n* (chosen *a priori*) different voltages by modifying the resistance "seen" by the PV system. Then, the related currents are measured together to the applied voltages and acquired by the ANN method, which provides the voltage to be set in order to obtain the MPP. In other words, these points (V_{PV}, I_{PV}) represent the input of the ANN, and the PV array voltage V_{EMMPA} related to the EMPPA, that is the global MPP esteemed only by the ANN, at the current operating conditions is the output of the ANN.

The working point (V_{EMMPA}, P_{EMPPA}) is thus imposed by the power converter to the PV array and subsequently the PS is activated to improve the accuracy of EMPPA, thus obtaining the EMPP. The main advantage of using the proposed method is the ability to predict the GMPP in a very short time, maintaining good accuracy even under different shading and environmental conditions. The time required by the ANN to predict the GMPP is strictly depending on the number, n, of sampling of the PV array, on the complexity of the ANN and on the hardware resources. In the following section a detailed description of the ANN based GMPP prediction and some quality indices useful to assess the goodness of the method are provided.

4. ANN based maximum power point prediction

An Artificial neural network is a computational model miming the biological neural network [43]. In such a model, a neuron is a processing unit that first linearly weighs the inputs, then elaborates the sum by means of an nonlinear function, called activation function (AF) and, finally, sends the results to the following neurons [44]. The model of a common neuron is given by the relationship (4), where z is the argument of the AF, as shown in Fig. 3:

$$z = \sum_{m=1}^{M} w_m x_m + \alpha \tag{4}$$

and $x_1, x_2, \ldots, x_M$ are the M incoming signals, and $w_1, w_2, \ldots, w_M$ are the related synapses weights.

Different AFs have been proposed in literature [45] such as threshold, linear and sigmoid transfer functions; the last one (5) is used in the case study.

$$y = \frac{1}{1 + e^{-z}} \tag{5}$$

Basically, the ANN can be represented by a directed graph where the nodes and the edges are, respectively, the neurons and the synapses [46]. Two different main kinds of ANN's structure arise from the way the neurons are connected to each other: feed-forward neural network (FNN) [47] and recurrent neural network (RNN) [48]. The structure of a multilayer FNN considered in the proposed application is depicted in Fig. 5, where the neurons of the input layer acts only as buffers for distributing the input signals (V_{PV}, I_{PV}). The output layer has one neuron providing the voltage value V_{EMMPA} corresponding to the EMPPA.

The considered ANN has been trained by using the back-propagation (BP) algorithm with the Levenberg-Marquardt optimization method [49], which is the most used supervised learning method for FNN. A supervised learning method [50] aims to train the ANN by providing it some combinations of desired solutions and the related value of the inputs. At first, the weights are, usually randomly, set. Then a supervised learning method is applied to properly modify the weights, in order to reduce the error between each desired output pattern and the solution provided by the ANN for the related input pattern. In the proposed application, at each stage of the learning process, the desired output pattern is the voltage value related to the GMPP and the input patterns are the values of V_{PV}, I_{PV} at the n points where the P–V characteristic is evaluated for a specific configuration of solar irradiance distribution and panels temperature. The patterns with an identical P–V curve could be gathered together to reduce the training period, that is when a pattern generates a curve identical to a pattern already used to train the ANN, use the curve again could be avoided in order to reduce the training time. On the other hand, the greater the number of patterns with an identical P–V curve, the greater the probability that similar scenarios occurs, and, consequently, the greater the probability that the ANN has to met the real GMPP in similar curves. The ANN should be able to find the real GMPP especially for the more probable scenarios in order to maximize the stored energy. Therefore, the use of all patterns to train the ANN aims to make it more suitable to correctly identify the real GMPP in PV curves frequently occurring, although this approach entails a greater training time.

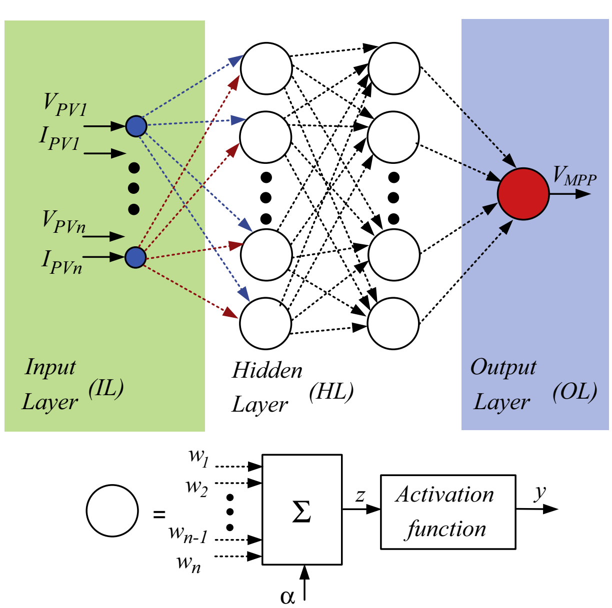

Fig. 3. Multilayer feed-forward neural network considered in the proposed application.

The ability of the entire method (ANN + PS) to correctly identify the real GMPP depends on the learning process as well as on the ANN's structure. The greater the number of couples (V_{PV}, I_{PV}) at which the P–V characteristic is evaluated the greater the probability that the EMPP approaches the real GMPP. On the other hand, a high number of measurements (V_{PV}, I_{PV}) to be evaluated implies a more complex network and, especially, involves a high time to track the GMPP variations. The performance of the entire method have to be computed for different ANN structures, by using always the same PS method, in order to support decision makers in the choice of the number of ingoing couples (V_{PV}, I_{PV}), the number of hidden layers and neurons per layer, which are suitable to provide the best tradeoff between the performance of the entire method and its computational burden. In this perspective, the following Performance Quality Indices (PQIs) are considered to assess the goodness of the solution provided by the entire MPPT method as well as by the ANN alone:

$$\mathrm{PQI}_1\ (\%) = \frac{100}{I}\sum_{i=1}^{I}\left(\frac{EMPP_i}{GMPP_i}\right) \tag{6}$$

$$\mathrm{PQI}_2\ (\%) = \frac{100}{I}\sum_{i=1}^{I} a_i \tag{7}$$

$$\mathrm{PQI}_3\ (\%) = 100\,\frac{\sum_{i=1}^{I}\left[a_i\left(\frac{EMPPA_i}{GMPP_i}\right)\right]}{\sum_{i=1}^{I} a_i} \tag{8}$$

$$\mathrm{PQI}_4\ (\%) = 100\,\frac{\sum_{i=1}^{I}\left[(1-a_i)\left(\frac{EMPP_i}{GMPP_i}\right)\right]}{I - \sum_{i=1}^{I} a_i} \tag{9}$$

where I is the number of tests executed to assess the performance, $GMPP_i$ is the global MPP when the i-th test is considered, $EMPP_i$ is the global MPP esteemed by the overall system when the i-th test is considered, $EMPPA_i$ is the global MPP esteemed only by the ANN when the i-th test is considered (that is, before the PS is applied); a_i is a constant equals to 1 if $EMPPA_i$ falls inside the same hill of the $GMPP_i$ when the i-th test is considered, otherwise it is equal to 0 (see Fig. 4).

The index PQI_1 gives a measure of the goodness of the $EMPP$ provided by the entire method with respect to the real GMPP value.

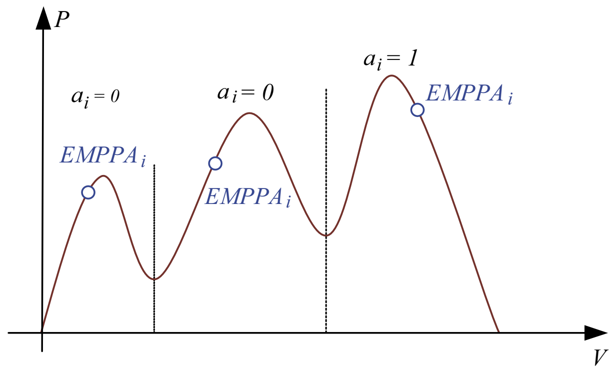

Fig. 4. Graphical explanation of the meaning of coefficient a_i.

The greater PQI_1 the better the average ability of the entire method to meet the real GMPP, e.g. PQI_1 equal to 100 means that global MPP esteemed by the overall system is always equal to the real one in all executed tests. PQI_2 is the percentage of times the *EMPPA* falls inside the hill of the GMPP. The greater PQI_2 the better the average ability of the ANN to provide to the PS a starting point (V_{EMMPA}, P_{EMMPA}), falling in the same "hill" where the real GMPP is located. The greater PQI_2 the lower the PS effort and, consequently, the time spent to reach the GMPP. The index PQI_3 gives a measure of the goodness of the *EMPPA* considering only when it falls inside the hill of the *GMPP*. The greater PQI_3 the better the average ability of the ANN to provide to the PS a starting point (V_{EMMPA}, P_{EMMPA}) close to the real GMPP, when this starting point falls inside the same GMPP's "hill".

An ANN does not work properly when it provides a starting point outside from the GMPP's "hill". On the other hand, if the peak of the hill where the PS operates has a similar amplitude than that where GMPP is located, the misleading solution provided by the ANN has a slightly negative effect on the performance of the entire method. In this regard, PQI_4 provides a measure of the goodness of the *EMPP* achieved by the entire procedure considering only when it falls outside from the hill of the GMPP.

PQI_1 and PQI_4 allow to indirectly compare the ANNs since they provide a measure of the goodness of the entire MPPT method. In particular, PQI_1 is the most significant since it provides information about the performance of the entire MPPT method when all the simulations are considered, whereas only a specific subset of simulations are considered for PQI_4. PQI_2 and PQI_3 directly measure the goodness of the ANN based MPPT method alone, but they lack on an overview on the performance of the entire MPPT method. On the other hand, an improvement on PQI_2, PQI_3 and PQI_4 positively affects PQI_1. In fact, PQI_1 encompasses as a whole all the aspects accounted by the other indices, so it provides the most complete information about how the performance of the entire method changes when the ANN's structure changes.

Hence, PQI_1 has to be used to identify the best ANN's structure. On the other hand, the other PQIs are useful anyway, since they enable the designer to grasp how much the different issues affect the ability of the entire method to meet the real GMPP.

The number of peaks in the *P–V* characteristic, their magnitudes, and the overall nature of the PV curve is strictly dependent on the temperature of each module composing the PV system, the insolation level, the shading pattern, and the array configuration [41]. The maximum number of hills in the *P–V* curve is related to the number of PV modules series connected, indicated in the following as *nos*. Hereafter, the minimum number of couples (V_{PV}, I_{PV}) is chosen equal to *nos*, thus the minimum number of input neurons is *2nos*. Actually, the number of input couples (V_{PV}, I_{PV}) is a performance parameter (objective function), since the greater this number, the greater the time needing to collect the input values of the ANN. Therefore, the number of couples (V_{PV}, I_{PV}) is both an optimization variable and a performance parameter. As a consequence, 2*nos* is the best solution in terms of response time, and it is expected to be the worst in terms of accuracy in the GMPP estimation.

As MPPT is a multimodal optimization problem, it involves to deal with a nonlinear function and, as it is well known, an ANN without hidden layer is not able to properly address a nonlinear function [51]. Hence, the ANN needs at least one hidden layer. A common method to size the hidden layer is to average the number of inputs and outputs [52]. Therefore, the minimum number of neurons in the hidden layer is chosen $nos + 1$ (by rounding up). By considering the minimum number of ANN's inputs and one hidden layer, the minimum number of synapses *mns* is given by:

$$mns = (2nos + 1)(nos + 1) \tag{10}$$

The performance of the proposed entire method is expected to enhance by increasing the number of input couples (V_{PV}, I_{PV}) and could also enhance by increasing the size and the number of hidden layers, involving the need on more computational resources. Hence, the number of synapses is also chosen as performance parameter (objective function), thus *mns* can be considered as the best solution from the computational burden point of view, but it is probably the worst in terms of MPPT method accuracy as it could provide the lowest PQI_1.

By tuning the optimization parameters, that are the number of input couples (V_{PV}, I_{PV}), the size and the number of hidden layers, a curve can be carried out for each performance parameter, that are the PQIs, the number of synapses as well as the number of (V_{PV}, I_{PV}) couples. When the curve related to a specific PQI is considered, e.g. PQI_1, and the curve related to the number of synapses and input couples are also considered, then a Pareto front can be carried out. A point on such a front is a tern made by: PQI_1 value, the number of ANN's input couples and synapses. As it is well known, there is not a point in a Pareto front better than another one; in fact, when two points of this front are compared, each one has at least one objective function value better and one worse than the other. It is worth to note that the number of ANN's input couples and synapses provide a time based comparison when no specific hardware solution is considered. The overall system response time will depend on the adopted hardware solutions and thus on the related cost the decision maker wants to face. Therefore, the decision maker chooses among these points the one that better complies with the specifications.

5. Case study

The effectiveness of the proposed GMPP searching method has been evaluated by considering a PV array consisting of two strings of three series ($nos = 3$) connected modules (2×3). This configuration could be installed on the roof of an electrical vehicle.

The technical specifications of PV modules under standard test conditions are reported in Table 1. Without loss of generality, the shading phenomenon on a PV module is modeled in Matlab by considering on it an uniform lower irradiance with respect to unshaded modules.

In order to evaluate the performances of the ANN based MPPT method, different ANN structures have been investigated. In particular, Table 2 reports the variation ranges related to the number of input *P–V* couples, the number of hidden layers and neurons in the first hidden layer (HL_1); hence 216 ANN structures have been investigated (exhaustive search).

The number of neurons in the hidden layers following the first one is chosen equal to half of neurons number in the previous one (by rounding up):

Table 1
Specification of PV modules.

Parameter	Value
V_{oc}	21.06 V
I_{sc}	3.80 A
Current at P_{max} (I_{MPP})	3.50 A
Voltage at P_{max} (V_{MPP})	17.10 V
Maximum power (P_{MPP})	59.90 W
V_{oc} coef. of temperature (K_V)	−0.084 V/°C
I_{sc} coef. of temperature (K_I)	3.3e^{-4} A/°C

Table 2
Range variations of the ANN design parameters.

Section	Minimum	Maximum
Input (V_{PV}, I_{PV}) couples	3	10
Number of HLs	1	3
Size of HL$_1$	4	20

$$Size\ (\mathrm{HL}_k) = 0.5 \cdot Size\ (\mathrm{HL}_{k-1}) \quad k \geqslant 2 \tag{11}$$

Many different shadowing factors, such as the height of other vehicles, buildings and any other obstacles, and their position with respect to the considered electric vehicle can simultaneously and partially affect the PV system of the vehicle moving in the traffic. Moreover, the shadowing pattern changes along the time since the position of the electric vehicle with respect to surrounding obstacles continuously changes while it moves in the traffic. Therefore, the set of data pattern employed to train the examined ANNs has been selected to cover the entire region where the they are expected to operate. In particular, the interval 0–1000 W/m^2 has been divided into six subintervals and the solar irradiance level in the center of each subinterval has been considered. Furthermore, ten temperature values between 10 and 55 °C have also been considered. The P–V characteristic curve obtained by means of Eqs. (1)–(3) has been carried out for each combination of the previous environmental operating conditions with all shading pattern combinations. In particular, $6^{2\times3}$ different solar irradiance combinations over the PV system has been considered to accounting for the aforementioned various shadowing conditions that can occur, and for each scenario 10 temperature levels (uniform along the system) has been considered. Therefore, each ANN has been trained by using 466,560, that are $6^{2\times3} \times 10$ combinations of data pattern. In particular, the input pattern (i.e. the values of V_{PV}, I_{PV}) for each ANN and the output pattern (i.e. the voltage value related to the GMPP), obtained from the characteristic curve, have been stored and provided to each ANN 500 times (that is the number of epochs) when the BP is applied.

After the training process has been completed, the PQIs have been evaluated by simulating 1000 randomly-generated different solar irradiances and temperatures, inside the same environmental ranges used at the train stage, so 216,000 simulations have been carried out. For each random simulation, the ANN estimates the optimal operating voltage V_{EMPPA}, providing the *EMPPA*, then, the PS is applied to obtain the V_{EMPP} related to the *EMPP*, and the PQIs are assessed. Whenever ANNs set negative voltage values or values greater than the open circuit voltage V_{oc}, the V_{EMPPA} is set to $0.77V_{co}$ [17]. It is worth to note that among all simulations, the ANN based MPPT method has set 0.1% times a negative voltage value and 0.02% times has set a value greater than the open circuit voltage V_{oc}.

Table 3 reports the extreme values of PQIs provided by the entire MPPT method and by the ANN alone, among the 216 simulated ANNs. In this case study, except for PQI$_4$, the ANNs with 3 input couples (V_{PV}, I_{PV}), 1 hidden layer with an high number of neurons (i.e. HL1 has a large size) achieve the worst performances.

Table 3
Best and worst PQIs values provided by the entire MPPT method or by considering only the ANN.

PQI (extreme)	Value (%)	Input couples	Number of HLs	Size of HL$_1$
PQI$_1$ (Best)	98.47	10	3	12
PQI$_1$ (Worst)	69.30	3	1	20
PQI$_2$ (Best)	96.40	10	3	12
PQI$_2$ (Worst)	67.94	3	1	16
PQI$_3$ (Best)	98.97	10	3	12
PQI$_3$ (Worst)	73.44	3	1	20
PQI$_4$ (Best)	94.50	9	3	12
PQI$_4$ (Worst)	42.96	9	1	8

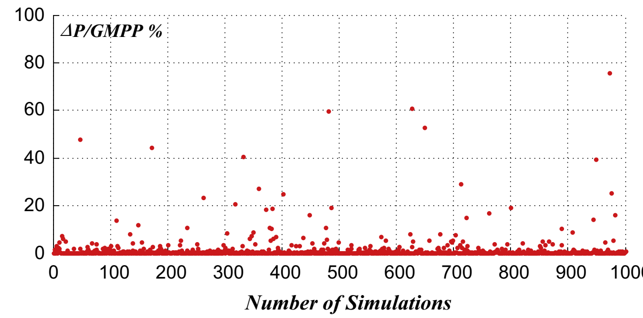

Fig. 5. Power error between EMPPA and GMPP in case of best PQI$_1$.

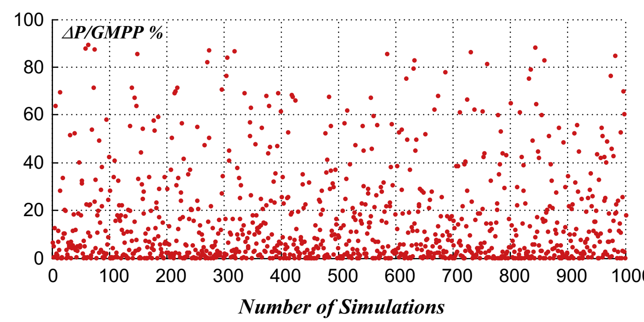

Fig. 6. Power error between EMPPA and GMPP in case of worst PQI$_1$.

Furthermore, it is worth noting the best performance are reached by using an high number of input (V_{PV}, I_{PV}) couples, 3 hidden layers and only a middle number of neurons.

Figs. 5 and 6 display the power error associated to the EMPPA in each simulation, when, respectively, the best and worst ANN configuration is considered. It is clearly visible that the implementation of a simple ANN structure provides a high number of false detection of the optimal operating condition, yielding to a considerably loss of extracted power from the PV system. On the contrary, this drawback is abundantly overcome when the best ANN configuration associated to PQI$_1$ is used.

Figs. 7–9 show the plots of the Pareto front as a scatter plot matrix [53]. This is a useful way to represent a 3-D Pareto front since each figure shows the value of a pair of objective functions for each solution. Moreover, the linear regression curve is reported as well. In particular, Figs. 7 and 8 show the tradeoff between the number of input P–V couples and synapses, respectively, against the values of PQI$_1$. The results bring to light that the greater the number of input P–V couples (and synapses) the better the PQI$_1$. Fig. 7 displays several optimal solutions for each input P–V couple because for a given input size, the ANN's performances can be sometimes improved by means of enlarging the size and/or the number of hidden layers. In fact, by tracing an horizontal line in

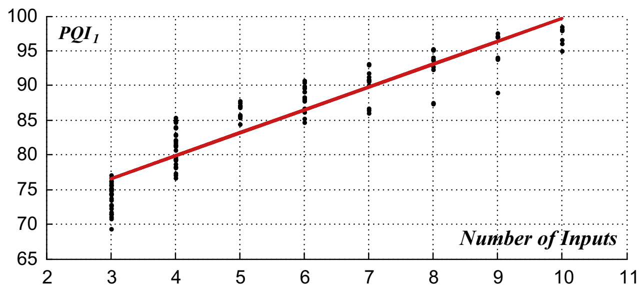

Fig. 7. Scatter plot matrix of the Pareto front: number of input vs PQI_1.

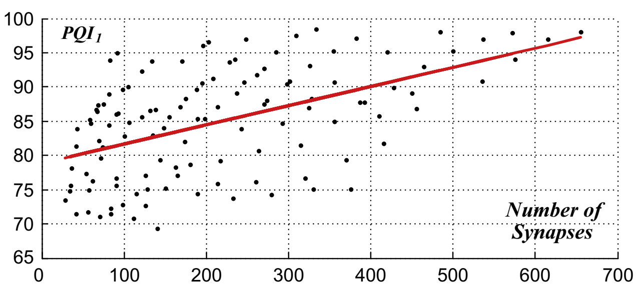

Fig. 8. Scatter plot matrix of the Pareto front: number of synapses vs PQI_1.

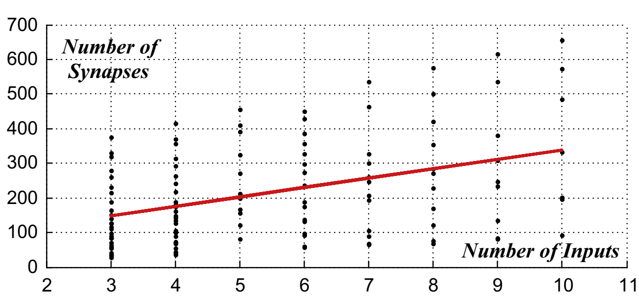

Fig. 9. Scatter plot matrix of the Pareto front: number of input vs number of synapses.

Table 4
Effect of parameter variations in the ANN with worst PQI_1.

PV specification		PQI_1	PQI_2	PQI_3	PQI_4
V_{oc}	I_{sc}	69.30	69.32	73.44	52.11
1.1 V_{oc}	I_{sc}	70.61	73.49	73.81	56.62
V_{oc}	1.1 I_{sc}	68.89	66.74	73.31	53.60
1.1 V_{oc}	1.1 I_{sc}	70.56	73.67	74.53	52.41
1.2 V_{oc}	I_{sc}	69.15	72.42	71.40	58.23
V_{oc}	1.2 I_{sc}	68.97	66.22	72.83	56.05
1.2 V_{oc}	1.2 I_{sc}	70.33	73.11	72.91	56.19
1.3 V_{oc}	I_{sc}	64.66	72.27	65.66	56.92
V_{oc}	1.3 I_{sc}	67.83	65.91	71.23	53.93
1.3 V_{oc}	1.3 I_{sc}	66.07	72.94	66.76	58.83

the figure it can be noticed that two ANNs with different input sizes can provide similar performances, by properly adopting an higher number of hidden layers and/or increasing their size.

Tables 4 and 5 report the effects of parameter variations on the estimation of GMPP. In particular, the performance of the proposed MPPT method has been evaluated by modifying till 30% two of the technical specifications of the PV modules: V_{oc} and I_{sc}. The results show that a considerable reduction of PQIs occurs when V_{oc} is

Table 5
Effect of parameter variations in the ANN with best PQI_1.

PV specification		PQI_1	PQI_2	PQI_3	PQI_4
V_{oc}	I_{sc}	98.47	96.40	98.97	84.98
1.1 V_{oc}	I_{sc}	95.59	93.50	96.65	80.25
V_{oc}	1.1 I_{sc}	98.23	96.30	98.75	84.82
1.1 V_{oc}	1.1 I_{sc}	95.55	94.20	97.05	71.10
1.2 V_{oc}	I_{sc}	78.41	73.30	86.46	56.31
V_{oc}	1.2 I_{sc}	98.02	95.80	98.47	87.73
1.2 V_{oc}	1.2 I_{sc}	81.88	79.10	89.18	54.27
1.3 V_{oc}	I_{sc}	75.14	71.80	80.28	62.05
V_{oc}	1.3 I_{sc}	97.52	95.00	98.31	82.41
1.3 V_{oc}	1.3 I_{sc}	74.28	70.10	80.72	59.17

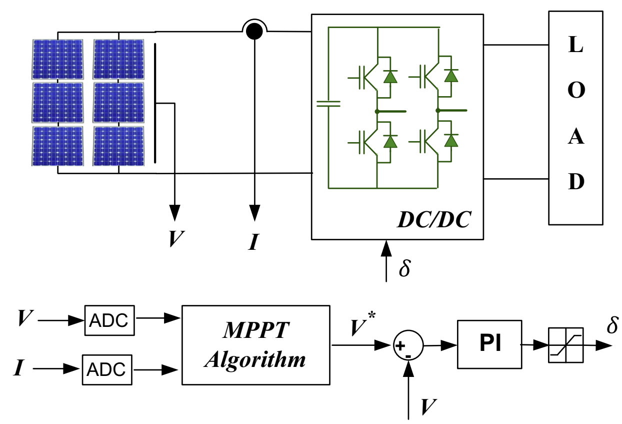

Fig. 10. Circuital scheme of the simulated PV system and block diagram of the control algorithm.

subjected to significant variations. On the contrary, variations of I_{sc} do not appreciably modify the performance of the proposed MPPT method.

Time varying simulations have been performed as well, by applying the proposed MPPT algorithm to the aforementioned PV array. In particular, the PV array was modeled by (1)–(3) and connected to a DC load by means of a DC–DC power converter. The operating point of the PV array has been modified by applying the proposed MPPT method and a closed loop voltage control. The duty cycle δ of the converter is modified according to the error between the desired V^* and measured V voltages. A circuital scheme of the PV system and a block diagram of the simulated control algorithm are shown in Fig. 10.

Dynamic response of the MPPT control algorithm applied to the same PV array configuration are shown in Figs. 11 and 12, considering two different ANN structures. The former ANN, indicated in the following as ANN1, has 4 input couples (V_{PV}, I_{PV}) and 2 hidden layers, the size of the first hidden layer is equal to 20. The second ANN, indicated as ANN2, differs from the former by only the number of input couples, which are 8.

The sequential simulations are performed assuming that $\Delta T = 5$ s, $\Delta P = 0.15$ P_{EMMP}, the operating point of the PV array is updated by the control system every 100 ms, and the shadowing pattern changes every 10 s. Initially, the system is at steady state at a given shadowing pattern whose GMPP is identified by $V_{PV} = 48$ V, $I_{PV} = 7.3$ A. At $t = 10$ s the procedure of Fig. 2 activates the ANN based MPPT algorithm due to the PV array is subjected to a different shadowing pattern that modifies the P–V curve and thus the GMPP. Similarly, at $t = 20$ s the ANNs are operated again. The figure displays the voltage, current and power of the PV array as well as the P–V curves associated to each shadowing pattern. The estimated MPP provided by ANN2 always converges to the real GMPP faster than ANN1 since the EMPPA provided by ANN2 is clo-

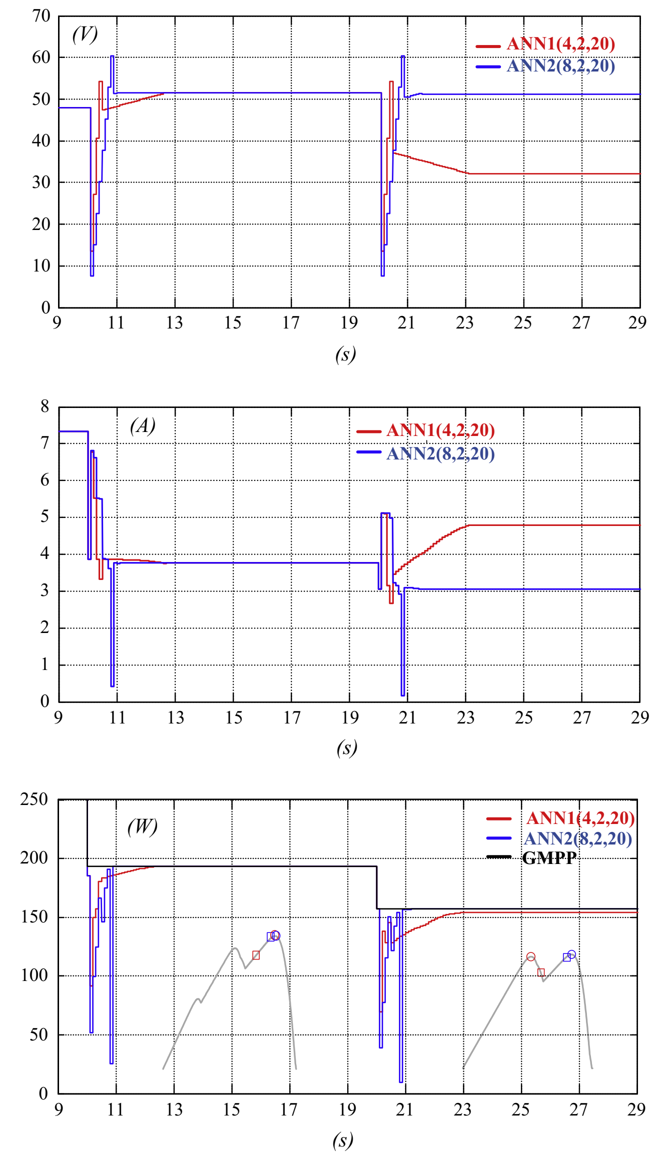

Fig. 11. Voltage, current and power at PV arrays terminals under two different shading patterns, when two different ANN structures are considered. The circles and the squares represent, respectively, the EMPP and EMPPA.

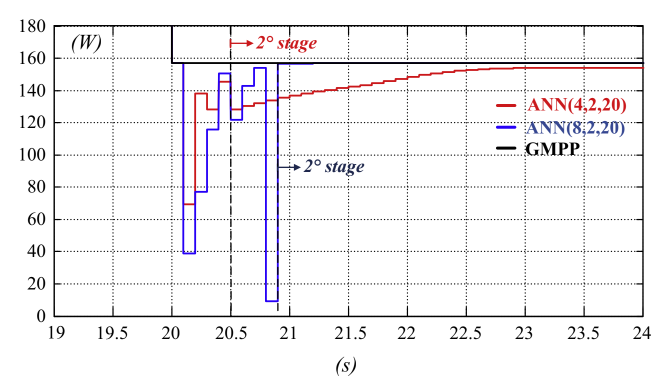

Fig. 12. Zoomed view of the second shadowing pattern displayed in Fig. 11.

ser to the GMPP. Therefore, when the considered sequence occurs, the second stage gives a more significant contribution if a small number of inputs are considered.

Furthermore, when the second shadowing pattern occurs, ANN1 provides an EMPPA located in a wrong "hill" of the *P–V* curve; therefore, the PS algorithm will move toward a suboptimal solution, yielding to a continuous little loss of energy even at steady state due to the erroneous identification of the MPP carried out by the ANN. It worth to note that these specific shadowing patterns have been chosen because they involve, especially the second one, a hard curve to deal with. Finally, the use of an enhanced PS, e.g. using a variable voltage step, or of a derivative algorithm can reduce the time necessary to reach the GMPP.

6. Conclusions and future work

The paper has presented a novel MPPT method that provides an accurate and fast estimation of the GMPP in a PV system subjected to continuous and rapidly changing shadowing patterns. Some quality indices have been proposed in order to compare the performance of different ANN structures and they have been computed in the case study considering numerous random generated scenarios. The results have also highlighted a good robustness of the method to parameter variations of PV system. In particular, this work have investigated, by means of a detailed analysis based on numerical simulations, the benefits of a novel implementation of a global MPPT algorithm, highlighting its effectiveness and suitability when applied to small PV systems installed, for instance, on the roof of electrical vehicles. In future works, experimental tests of the proposed MPPT could highlight which hardware solutions are more suitable also considering the economical investment point of view. In particular, the trade-off among implementation costs and energy losses could be investigated.

References

[1] Esram T, Chapman PL. Comparison of photovoltaic array maximum power point tracking techniques. IEEE Trans Energy Convers 2007;22(2):439–49.
[2] De Brito MAG, Galotto L, Sampaio LP, de Azevedo e Melo G, Canesin CA. Evaluation of the main MPPT techniques for photovoltaic applications. IEEE Trans Indus Electr 2013;60(3):1156–67.
[3] Ishaquea K, Salamb Z. A review of maximum power point tracking techniques of PV system for uniform insolation and partial shading condition. Renew Sustain Energy Rev 2013;19(March):475–88.
[4] Jain S, Agarwal V. Comparison of the performance of maximum power point tracking schemes applied to single-stage grid-connected photovoltaic systems. IET Electr Power Appl 2007;1(5):753–62.
[5] Femia N, Granozio D, Petrone S, Spagnuolo G, Vitelli M. Predictive & adaptive MPPT perturb and observe method. IEEE Trans Aerosp Electron Syst 2007;43(3):934–50.
[6] Casadei D, Grandi G, Rossi C. Single-phase single-stage photovoltaic generation system based on a ripple correlation control maximum power point tracking. IEEE Trans Energy Convers 2006;21(2):562–8.
[7] Abdelsalam AK, Massoud AM, Ahmed S, Enjeti P. High-performance adaptive perturb and observe MPPT technique for photovoltaic-based microgrids. IEEE Trans Power Electron 2011;26(4):1010–21.
[8] Qiang M, Mingwei S, Liying L, Guerrero JM. A novel improved variable step-size incremental-resistance MPPT method for PV systems. IEEE Trans Industr Electron 2011;58(6):2427–34.
[9] Fangrui L, Shanxu D, Fei L, Bangyin L, Yong K. A variable step size INC MPPT method for PV systems. IEEE Trans Industr Electron 2008;55(7):2622–8.
[10] Sera D, Teodorescu R, Hantschel J, Knoll M. Optimized maximum power point tracker for fast-changing environmental conditions. IEEE Trans Industr Electron 2008;55(7):2629–37.
[11] Weidong X, Ozog N, Dunford WG. Topology study of photovoltaic interface for maximum power point tracking. IEEE Trans Industr Electron 2007;54(3):1696–704.
[12] Karlisa AD, Kottasb TL, Boutalisb YS. A novel maximum power point tracking method for PV systems using fuzzy cognitive networks (FCN). Electric Power Syst Res 2007;77(3–4):315–27.
[13] Kulaksız AA, Akkaya R. A genetic algorithm optimized ANN-based MPPT algorithm for a stand-alone PV system with induction motor drive. Sol Energy 2012;86(9):2366–75.
[14] Bahgata ABG, Helwab NH, Ahmadb GE, El Shenawyb ET. Maximum power point traking controller for PV systems using neural networks. Renew Energy 2005;30(8):1257–68.
[15] Hiyama T, Kitabayashi K. Neural network based estimation of maximum power generation from PV module using environmental information. IEEE Trans Energy Convers 1997;12(3):241–7.

[16] Salah CB, Ouali M. Comparison of fuzzy logic and neural network in maximum power point tracker for PV systems. Electric Power Syst Res. 2011;81(1):43–50.
[17] Elobaid LM, Abdelsalam AK, Zakzouk EE. Artificial neural network based maximum power point tracking technique for PV systems. In: Proc of 38th annual conference on IEEE industrial electronics society, IECON; 2012. p. 937–42.
[18] Chiu YH, Luo YF, Huang JW, Liu YH. An ANN-based maximum power point tracking method for fast changing environments. In: Proc of 13th international symposium on advanced intelligent systems; 2012. p. 715–20.
[19] Seo JH, Im CH, Heo CG, Kim JK, Jung HK, Lee CG. Multimodal function optimization based on particle swarm optimization. IEEE Trans Magn 2006;42(4):1095–8. http://dx.doi.org/10.1109/TMAG.2006.871568.
[20] Miyatake M, Veerachary M, Toriumi F, Fujii N, Ko H. Maximum power point tracking of multiple photovoltaic arrays: a PSO approach. IEEE Trans Aerosp Electron Syst 2011;47(1):367–80.
[21] Koutroulis E, Blaabjerg F. A new technique for tracking the global maximum power point of PV arrays operating under partial-shading conditions. IEEE J Photovoltaics 2012;2(2):184–90.
[22] Nguyen TL, Low K-S. A global maximum power point tracking scheme employing DIRECT search algorithm for photovoltaic systems. IEEE Trans Industr Electron October 2010;57(10):3456–67.
[23] Ji YH, Jun DY, Kim JG, Kim JH, Lee TW, Won CY. A real maximum power point tracking method for mismatching compensation in PV array under partially shaded conditions. IEEE Trans Power Electron 2011;26(4):1001–9.
[24] Patel H, Agarwal V. Maximum power point tracking scheme for PV systems operating under partially shaded conditions. IEEE Trans Ind Electron 2008;55(4):1689–98.
[25] Boztepe M, Guinjoan F, Velasco-Quesada G, Silvestre S, Chouder A, Karatepe E. Global MPPT scheme for photovoltaic string inverters based on restricted voltage window search algorithm. IEEE Trans Industr Electron 2014;61(7):3302–12.
[26] Syafaruddin, Karatepe E, Hiyama T. Artificial neural network-polar coordinated fuzzy controller based maximum power point tracking control under partially shaded conditions. IET Renew Power Gener 2009;3(2):239–53.
[27] Alajmi BN, Ahmed KH, Finney SJ, Williams BW. A maximum power point tracking technique for partially shaded photovoltaic systems in microgrids. IEEE Trans Industr Electron 2013;60(4):1596–606.
[28] Peng L, Yaoyu L, Seem JE. Sequential ESC-based global MPPT control for photovoltaic array with variable shading. IEEE Trans Sustain Energy 2011;2(3):348–58.
[29] Kazmi S, Goto H, Ichinokura O, Guo Hai-Jiao. An improved and very efficient MPPT controller for PV systems subjected to rapidly varying atmospheric conditions and partial shading. In: Proc of the Australasian power engineering conference; 2009. p. 1–6.
[30] Ahmed J, Salam Z. A maximum power point tracking (MPPT) for PV system using Cuckoo Search with partial shading capability. Appl Energy 2014;119(15):118–30.
[31] Mamarelis E, Petrone G, Spagnuolo G. A two-steps algorithm improving the P&O steady state MPPT efficiency. Appl Energy 2014;113(January):414–21.
[32] Punitha K, Devaraj D, Sakthivel S. Artificial neural network based modified incremental conductance algorithm for maximum power point tracking in photovoltaic system under partial shading conditions. Energy 2013;62(1):330–40.
[33] Ishaque K, Salam Z, Shamsudin A, Amjad M. A direct control based maximum power point tracking method for photovoltaic system under partial shading conditions using particle swarm optimization algorithm. Appl Energy 2012;99(April):414–22.
[34] Ghosh A, Dehuri S. Evolutionary algorithms for multi-criterion optimization: a survey. Int J Comput Inform Sci 2004;2(1):38–57.
[35] Daraban S, Petreus D, Morel C. A novel global MPPT based on genetic algorithms for photovoltaic systems under the influence of partial shading. In: 39th annual conference of the IEEE industrial electronics society, IECON; 2013.
[36] Sareni B, Krahenbuhl L. Fitness sharing and niching method revisited. IEEE Trans Evol Comput 1998;2(3):97–106. http://dx.doi.org/10.1109/4235.735432.
[37] Hooke R, Jeeves TA. Direct search solution of numerical and statistical problems. J Assoc Comput Mach 1961;8(2):212–29.
[38] Dilettoso E, Rizzo SA, Salerno N. A parallel version of the self-adaptive low-high evaluation evolutionary-algorithm for electromagnetic device optimization. IEEE Trans Magn 2014;50(2):633–6. http://dx.doi.org/10.1109/TMAG.2013.2284928.
[39] Liu YH, Chen JH, Huang JW. Global maximum power point tracking algorithm for PV systems operating under partially shaded conditions using the segmentation search method. Sol Energy 2014;103(May):350–63.
[40] Karatepe E, Boztepe M, Colak M. Development of a suitable model for characterizing photovoltaic arrays with shaded solar cells. Sol Energy 2007;81(8):977–92.
[41] Patel H, Agarwal V. MATLAB-based modeling to study the effects of partial shading on PV array characteristics. IEEE Trans Energy Convers 2008;23(1):302–10.
[42] Liu YH, Chen JH, Huang JW. A review of maximum power point tracking techniques for use in partially shaded conditions. Renew Sustain Energy Rev 2015;41(January):436–53.
[43] Singh Y, Chauhan AS. Neural networks in data mining. J Theor Appl Inform Technol 2009;5(6):36–42.
[44] McCulloch WS, Pitts W. A logical calculus of the ideas imminent in nervous activity. Bull Math Biophys 1943;5:115–33. http://dx.doi.org/10.1007/BF02478259.
[45] Jain AK, Mao J, Mohiuddin KM. Artificial neural networks: a tutorial. Computer 1996;29:31–44. http://dx.doi.org/10.1109/2.485891.
[46] Podolak IT. Functional graph model of a neural network. IEEE Trans Syst Man Cybern B Cybern 1998;28(6):876–81. http://dx.doi.org/10.1109/3477.735398.
[47] Tascikaraoglu A, Erdinc O, Uzunoglu M, Karakas A. An adaptive load dispatching and forecasting strategy for a virtual power plant including renewable energy conversion units. Appl Energy 2014;119(15):445–53. http://dx.doi.org/10.1016/j.apenergy.2014.01.020.
[48] Farahani M. A multi-objective power system stabilizer. IEEE Trans Power Syst 2013;28(3):2700–7. http://dx.doi.org/10.1109/TPWRS.2012.2227980.
[49] Rumelhart DE, Hinton GE, Williams RJ. Learning representations by back-propagating errors. Nature 1986;323:533–6. http://dx.doi.org/10.1038/323533a0.
[50] Mellita A, Kalogirou SA. Artificial intelligence techniques for photovoltaic applications: a review. Prog Energy Combust Sci 2008;34:574–632. http://dx.doi.org/10.1016/j.pecs.2008.01.001.
[51] Haykin S. Neural networks: a comprehensive foundation. New York: Macmillan; 1994.
[52] Piramuthu S, Shaw MJ, Gentry JA. A classification approach using multi-layered neural networks. Decis Support Syst 1994;11(5):509–25.
[53] Deb K. Optimization using evolutionary algorithms, chichester. U.K.: Wiley; 2001.